ORIGINAL ARTICLE

Arquivos Brasileiros de Oftalmologia

Clinical features and corneal optical anisotropies in a rabbit model of limbal stem cell deficiency

Fenótipos clínicos e anisotropias ópticas da córnea em coelhos com deficiência de células tronco limbais

Karina Kamachi Kobashigawa[1], Marcela Aldrovani[1], Alexandre A. F. Barros Sobrinho[1], Paloma do Espírito Santo Silva[1], Paulo F. Marcusso[2], Fausto A. Marinho-Neto[2], Ivan R. Martines Padua[1], José Luiz Laus[1]

1. Departamento de Clínica e Cirurgia Veterinária, Faculdade de Ciências Agrárias e Veterinárias, Universidade Estadual Paulista, Jaboticabal, SP, Brasil.
2. Departamento de Patologia Veterinária, Faculdade de Ciências Agrárias e Veterinárias, Universidade Estadual Paulista, Jaboticabal, SP, Brasil.

ABSTRACT | Purposes: To investigate the intra-laboratory reproducibility of clinical features and to evaluate corneal optical anisotropies in a rabbit model of limbal stem cell deficiency. **Methods**: Limbal injury was induced in the right eye of 23 adult New Zealand White rabbits using a highly aggressive protocol that combined 360 degrees limbal peritomy, keratolimbectomy, alkaline chemical burn, and mechanical removal of the epithelium. Clinical evaluation of the injured eyes was performed for 28 days and included corneal impression cytology. Corneas with a severe clinical outcome set typical of limbal stem cell deficiency were then collected, subjected to a histopathological examination, and examined for optical anisotropies. Corneas from healthy rabbit eyes were used as controls. Differences in optical path due to stromal collagen birefringence, as well as linear dichroism related to the expression and spatial orientation of glycosaminoglycan chains from proteoglycans, were measured from cross-sections under a quantitative polarized light microscope. **Results:** One eye showed signs of hypopyon and was excluded. Signs of ocular inflammation were observed in all eyes studied (n=22). Corneal impression cytology did not detect goblet cells. Twelve of the 22 corneas presented a clinical outcome set typical of limbal stem cell deficiency, which is characterized by the presence of epithelial defects, inflammatory cells, moderate-to-severe opacity, and neovascularization. Microscopic studies under polarized light revealed that relative to controls, limbal stem cell deficiency caused a 24.4% increase in corneal optical path differences. Further, corneas with limbal stem cell deficiency were less dichroic than controls. **Conclusions:** These results suggest that rabbit models of limbal stem cell deficiency must be rigorously screened for use in preclinical studies to ensure experimental homogeneity because protocols used to create limbal stem cell deficiency could be not associated with good intra-laboratory reproducibility of clinical features. Limbal stem cell deficiency, as induced herein, altered the optical anisotropic properties of the corneal stroma. Such alterations are indicative of changes in collagen packing and the spatial orientation of glycosaminoglycan chains from proteoglycans. Knowledge of these changes is important to potentiate strategies aimed at restoring the morphofunctional integrity of the corneal stroma affected by limbal stem cell deficiency.

Keywords: Birefringence; Corneal stroma; Anisotropy; Stem cells; Limbus corneae; Glycosaminoglycans

RESUMO | Objetivos: Investigar a reprodutibilidade intra-laboratorial dos fenótipos clínicos e avaliar anisotropias ópticas em córneas de coelhos com deficiência de células tronco limbais. **Métodos**: Lesões ao limbo foram feitas no olho direito de 23 coelhos adultos da Nova Zelândia Branco, usando um protocolo altamente agressivo, que envolveu peritomia limbal em 360 graus, ceratolimbectomia, cauterização por álcali, e remoção mecânica de epitélio remanescente. Os olhos foram clinicamente avaliados por 28 dias, inclusive por citologia de impressão corneal. As córneas que manifestaram um conjunto de alterações típicas de deficiência de células tronco limbais foram coletadas e submetidas à estudos em histopatologia e em anisotropias ópticas. Córneas saudáveis foram usadas como controles. Diferenças de caminho óptico de birrefringência relacionada à organização do colágeno estromal, e dicroísmo linear relacionado à expressão e à orientação das cadeias de glicosaminoglicanos dos proteoglicanos estromais, foram quantificados por microscopia de luz polarizada. **Resultados**: Um olho apresentou hipópio e foi excluído do

Submitted for publication: October 20, 2017
Accepted for publication: February 16, 2018

Funding: This study was supported by Fundação de Auxílio à Pesquisa de São Paulo (FAPESP Proc. 2012/17308-5 and 2013/01494-7, and 2014/18007-4), and Conselho Nacional de Desenvolvimento Científico e Tecnológico (CNPq Proc. 467289/2014-0).

Disclosure of potential conflicts of interest: None of the authors have any potential conflict of interest to disclose.

Corresponding author: Marcela Aldrovani.

Unidade de Oftalmologia. Departamento de Clínica e Cirurgia Veterinária. Faculdade de Ciências Agrárias e Veterinárias. Universidade Estadual Paulista. Via de acesso Prof. Paulo Donato Castellane km 5 - Jaboticabal, SP - 14884-900 Brazil
E-mail: marcela.aldrovani@gmail.com

Approved by the following research ethics committee: Universidade Estadual Paulista (# 05429/14).

This content is licensed under a Creative Commons Attributions 4.0 International License.

estudo. Todos os olhos estudados (n=22) apresentaram sinais de inflamação ocular. A citologia de impressão não detectou células caliciformes na superfície corneal. Doze de 22 córneas manifestaram alterações clínicas típicas de deficiência de células tronco limbais, caracterizado por defeitos epiteliais, infiltrados inflamatórios, opacidade de moderada à severa, e neovascularização. Estudos por microscopia de luz polarizada mostraram que a deficiência de células tronco limbais aumentou a diferenças de caminho óptico corneal em 24,4% (versus controles). As córneas com deficiência de células tronco limbais foram menos dicroicas do que as córneas controle. **Conclusões**: Coelhos com deficiência de células tronco limbais, para aplicações em estudos pré-clínicos, devem ser rigorosamente selecionados para assegurar homogeneidade experimental, pois há evidências de que protocolos utilizados para indução de deficiência de células tronco limbais não estão associados com boa reprodutibilidade intra-laboratorial de fenótipos clínicos. A deficiência de células tronco limbais, como induzida aqui, alterou as propriedades ópticas anisotrópicas do estroma corneal. Tais alterações são indicativas de mudanças no empacotamento de colágeno e na orientação das cadeias de glicosaminoglicanos dos proteoglicanos. Conhecimentos nessas alterações são importantes para potencializar estratégias que visam a restabelecer a integridade morfofuncional do estromal corneal acometido pela deficiência de células tronco limbais.

Descritores: Birrefringência; Substância própria; Anisotropia; Células-tronco; Limbo da córnea; Glicosaminoglicanos

INTRODUCTION

The corneal surface is formed by a specialized type of epithelial cells that undergo continuous renewal from stem or progenitor cells located in the basal limbal epithelium[1]. Loss of these limbal stem/progenitor cells allows colonization of the corneal epithelium by conjunctival cells. This process is usually referred to as limbal stem cell deficiency (LSCD)[2,3]. Surgical reconstruction of the ocular surface with LSCD is difficult and may require the involvement of cell therapy procedures[4,5].

Studies on cell therapies for LSCD are usually conducted using rabbit eyes[4,5]. However, many authors do not report whether the protocol used to induce LSCD in rabbits results in the production of lesions with good reproducibility of clinical features. Furthermore, while epithelial defects associated with rabbit LSCD have been reported, there is little information on changes in the stromal macromolecular environment.

The corneal stroma is predominantly composed of extracellular matrix (ECM), which gives the cornea important optical anisotropic properties whose molecular origin is the same of transparency, refractive index, and biomechanics of cornea[6,7]. Optical anisotropies are closely related to the macromolecular composition of the stromal environment and provide input on the orientation and ordering of collagen fibers (CFs) and proteoglycans (PGs)[8,9]. Given this close relationship, many diseases accompanied by stromal dysfunction, such as keratoconus and pterygium, have been evaluated by assessing changes in anisotropy[10,11]. There is evidence to suggest a correlation between clinical-pathological features and optical anisotropic properties of damaged corneas[10,11].

The cornea simultaneously manifests two types of anisotropies, which lead to changes in the polarization of light. These two types are birefringence and linear dichroism (LD)[6,7]. Birefringence is an anisotropy related to changes in the phases of the components of the polarized electric vector[6]. It can be evaluated and quantified, in terms of optical path difference (OPD), from histological sections using a second harmonic generation microscope[12] or a quantitative polarized light microscope equipped with phase compensators[6]. LD is an anisotropy of spectral absorption and is characterized by changes in the amplitude of the components of the polarized electric vector,[6,7] which can be quantified using spectrophotometric techniques once samples have been stained using thiazine (e.g., toluidine blue, TB) or azo (e.g., ponceau SS) dyes[6,7].

In this study, we tested the hypothesis that protocols intended to induce LSCD in rabbits do not have good intra-laboratory reproducibility of clinical phenotypes and that LSCD alters corneal optical anisotropies. The protocol used to destroy the ocular surface herein is one of the most aggressive described in the literature[13]. Following injury, the eyes were then studied for 28 days. At the end, corneas presenting a clinical outcome set typical of LSCD were evaluated for birefringence and LD.

METHODS

Animal use and ethical approval

This study adhered to the guidelines of the Association for Research in Vision and Ophthalmology (ARVO) and its statement on the use of animals in ophthalmic research. The entire research protocol was approved by the Ethics Committee on Animal Use (Protocol No. 05429/14) FCAV/Unesp.

Adult New Zealand White rabbits of both genders that weighed from 2 kg to 2.5 kg were used in the research. All were free from ophthalmic and systemic disorders.

Surgical procedures to induce LSCD

The induction of LSCD in rabbits (n=23) was performed under general anesthesia with isoflurane (Cristália). Morphine (Cristália) was given as a preanesthetic medication, and topical tetracaine ophthalmic drops containing 0.1% phenylephrine (Allergan, São Paulo, Brazil) were applied before the procedure.

LSCD was induced according to a protocol described by Andrade et al.[13]. Eyes were subjected to radical 360 degrees limbal peritomy and keratolimbectomy. Then, a 1.5-cm-diameter filter paper (Millipore, Darmstadt, Germany) soaked in an aqueous 0.5 M NaOH solution was positioned on the axial region of the cornea for 1 min. After that, the same filter paper was used to scarify the cornea for 1 min; then, the eye was washed with 0.9% NaCl. Remnant epithelial cells were mechanically removed using a sterile #15 blade[13]. A fluorescein dyeing test was performed within 24 h following surgery and demonstrated that all regions of each cornea had epithelial defects.

Postoperative care included the instillation of tobramycin eye drops (Alcon, São Paulo, Brazil) every 6 h for 4 days, and subcutaneous tramadol (Cristália) injections were administered every 12 h for 4 days.

Ocular clinical examination

The injured eyes were monitored using slit-lamp examination (Kowa, Tokyo, Japan) and fluorescein staining (Ophthalmos, São Paulo, Brazil). Photographic images were taken on days 3, 7, 14, 21, and 28. Chemosis, blepharospasm, ocular discharge, and conjunctival hyperemia were scored as Grade 0, no sign; Grade 1, mild; Grade 2, moderate; and Grade 3, severe, according to previously published criteria[13].

Corneal transparency was evaluated and scored as Grade 0, totally clear; Grade 1, mild opacity, able to observe details on the iris; Grade 2, moderate opacity, unable to observe details on the iris; and Grade 3, severe dense opacity completely obscuring the pupil contour[13].

Corneal ulcers (positive fluorescein) and neovascularization areas were quantified using ImageJ software (http://imagej.nih.gov/ij/; National Institutes of Health, Bethesda, MD, USA)[14,15].

An ocular clinical feature, as characterized by the concomitant presence of diffuse corneal epithelial defects, moderate-to-severe corneal opacification, and neovascularization, was considered to be related to LSCD[16].

Corneal impression cytology (IC)

Corneal IC was used to monitor the emergence of conjunctival goblet cells over the cornea. A circular disc of cellulose acetate membrane filter paper (Millipore, Bedford, MA, USA) was placed on the central ocular surface. After the paper was pressed for 20 s with constant pressure, it was gently lifted, air dried, fixed with 4% paraformaldehyde (Dinâmica, São Paulo, Brazil), and stained with periodic acid-Schiff[16].

Tissue processing

Rabbits were euthanized via sodium thiopental (Cristália, Itapira, Brazil) and corneas with LSCD were harvested, fixed by immersion in 10% buffered formalin (Dinâmica, São Paulo, Brazil), processed for routine inclusion in paraffin (Merck, Darmstadt, Germany), and sectioned using a microtome (7 µm thickness). Five corneas harvested from healthy eyes were also processed and used as controls. Paraffin embedding has no impact on optical anisotropies of CFs[6].

Two sections from each cornea were stained with 0.025% TB (Sigma-Aldrich, St. Louis, MO, USA) in 0.1 M McIlvaine buffer, pH 4.0, for 15 min[17]. These samples were mounted in Canada natural balsam (Vetec, Rio de Janeiro, Brazil) and used to assess the histopathological conditions of corneas with LSCD and to study LD.

Measurements of optical anisotropies

Birefringence

Theory. When corneal tissue is illuminated with polarized light, the orthogonal components of the electric vector display two refractive indices that lead to light propagation at different speeds and directions[6,7,17]. The vector components experience a phase shift relative to each another, which is represented by the equation $\delta=(2\pi/\lambda)L\Delta_n$, where δ is the phase shift between propagating orthogonal polarizations, λ is the light wavelength in vacuum, L is the thickness of the sample, and Δ_n is the difference in refractive indices between the two optical axes of the anisotropic sample[6]. $L\Delta_n$ is known as the OPD.

Experimental setup. Unstained tissue section slides (two from each cornea) were soaked in water (refractive index of 1.333) for 1 h[6]. Birefringence was examined using an Olympus BX-53 polarized light microscope (Tokyo, Japan) equipped with UPLFLN 20/0.75 objective, rotating stage, a 100-W halogen lamp, monochromatic light of 546 nm, and a Sénarmont compensator consisting of a quarter wavelength retardation plate (Figure 1)[6]. The angle of phase differences read by the compensator was multiplied by 3.03 to establish the OPD. During the examinations, the long axis of the corneal section was continually maintained at 45 degrees relative to the

plane of the polarized light (PPL)[6,17]. Sixty OPD measurements were made for each research group (corneas with LSCD vs. controls).

LD

LD was studied in TB-stained samples (two from each cornea) with the same microscope used to evaluate birefringence. The analyzer filter was removed from the light path[6,7,17]. Spectral absorptions were sequentially assessed using photon wavelengths of 480, 500, 520, 540, 560, 580, and 600 nm, which were obtained with narrow-bandpass interference filters (Edmund Industrial Optics, Barrington, NJ, USA). For each wavelength, the long axis of the corneal section was positioned both perpendicular ($A^{\perp}$) and parallel ($A\parallel$) to the PPL[6,7,17]. Absorption measurements (60 per group), in arbitrary units, were performed using ImageJ software calibrated in the optical density mode. The slide's background was used to calibrate the system (100% transmittance). Spectral absorption curves were constructed by plotting the mean absorbance values, $A\parallel$ and $A^{\perp}$, versus the photon wavelengths. LD values were calculated at the maximum absorbance points of the curves, using the $A\parallel - A^{\perp}$ formula described previously[6,7,17].

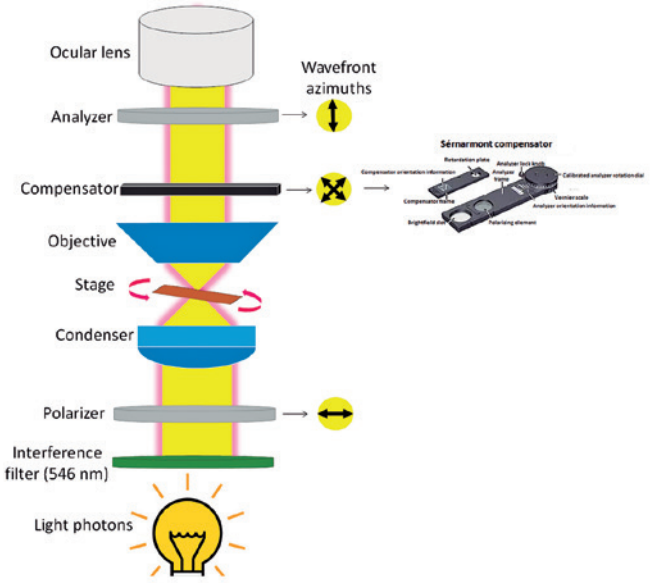

Figure 1. Schematic diagram of the major parts of a quantitative polarized light microscope. This microscope is designed to observe anisotropic materials. It is equipped with UPLFLN objectives, an analyzer (placed in the optical pathway between the objective rear aperture and the observation tubes or camera port), a polarizer (positioned in the light path before the specimen), a rotating stage, a 100-W halogen lamp, a 546-nm monochromatic light, and a Sénarmont compensator with a quarter wavelength retardation plate. The microscopic image contrast arises from the interaction of plane polarized light with the anisotropic sample to produce two individual wave components that are polarized in mutually perpendicular planes. In relation to the Sénarmont compensation technique, the rotation of the polarized light microscope analyzer through 180 degrees is equivalent to a relative specimen retardation value of one wavelength (when monochromatic light is employed). As the analyzer is rotated through its full 180 degree range, a birefringent specimen appears alternately dark or bright at 90 degree intervals.

Data analyses

Categorical variables were analyzed using the chi-square test and Wilcoxon signed-ranks test. Quantitative variables were compared using the unpaired Student's *t*-test, one-way repeated measures analysis of variance (ANOVA), and Tukey's post-hoc test when appropriate. Differences with $p<0.05$ were considered significant. All comparisons were performed using commercially available software (Minitab, State College, San Diego, CA, USA).

RESULTS

Clinical features

One eye exhibited signs of hypopyon and was excluded from the study. Chemosis, blepharospasm, discharge, and hyperemia were observed in all studied eyes (n=22) (Table 1), and each was more severe in the first week of postoperative (Table 2). All corneas showed severe dense opacity (Grade 3), which was most prominent on days 21 and 28.

Corneal vessels were observed in all eyes from the seventh postoperative day. Persistent and diffuse epithelial defects were observed in 20 eyes (90.90%). The evolutions of corneal ulcers and neovascularization areas over time are presented in figure 2A and B. The mean percentage of the ulcerated corneal area decreased over time (mean, 38.65% at day 28; range, 4.76-81.81%). In contrast, the mean percentage of the corneal area covered by vessels increased (mean, 55.10% at day 28; range, 12.0-77.5%).

Table 1. Ocular clinical features in a rabbit model of LSCD

	Evaluation times				
Clinical signs	Day 3	Day 7	Day 14	Day 21	Day 28
Chemosis	100.0[a]	100.0[a]	36.3[b]	---	---
Blepharospasm	100.0[a]	100.0[a]	68.1[a]	22.7[b]	---
Ocular discharge	95.4[a]	95.4[a]	95.4[a]	50.0[b]	45.4[b]
Conjunctival hyperemia	100.0[a]	100.0[a]	81.8[a]	50.0[b]	36.3[b]

LSCD= limbal stem cell deficiency.
Data are presented as percentage.
Statistical differences were significant when $p<0.05$.
Different letters in the same line represent statistical differences.
---= no sign.

At day 28, 12 eyes presented with a clinical outcome set typical of LSCD, characterized by the presence of epithelial defects, moderate-to-severe corneal opacity, and corneal neovascularization.

Table 2. Ocular clinical features in a rabbit model of LSCD

	Clinical signs				
	Chemosis				
Evaluation times	Grade 0	Grade 1	Grade 2	Grade 3	p value
					<0.001
Day 3	0	7	11	4	
Day 7	0	9	13	0	
Day 14	15	5	2	0	
Day 21	21	1	0	0	
Day 28	22	0	0	0	
	Blepharospasm				
	Grade 0	Grade 1	Grade 2	Grade 3	p value
					<0.001
Day 3	0	5	10	7	
Day 7	0	7	14	1	
Day 14	5	15	2	0	
Day 21	14	5	0	3	
Day 28	21	1	0	0	
	Ocular discharge				
	Grade 0	Grade 1	Grade 2	Grade 3	p value
					<0.001
Day 3	0	2	12	8	
Day 7	2	14	4	2	
Day 14	4	17	0	1	
Day 21	9	11	2	0	
Day 28	10	11	1	0	
	Conjunctival hyperemia				
	Grade 0	Grade 1	Grade 2	Grade 3	p value
					<0.01
Day 3	0	0	4	18	
Day 7	0	0	9	13	
Day 14	7	9	3	3	
Day 21	11	6	2	3	
Day 28	17	5	0	0	
	Corneal transparency/opacity				
	Grade 0	Grade 1	Grade 2	Grade 3	p value
					<0.01
Day 3	0	21	1	0	
Day 7	0	20	2	0	
Day 14	3	14	4	1	
Day 21	3	9	6	3	
Day 28	3	5	7	6	

LSCD= limbal stem cell deficiency.
Data are presented as numbers.
Clinical features were studied from 22 eyes as one eye was excluded from the study (as it showed signs of hypopyon).

Corneal IC

Corneal IC showed inflammatory cells in the corneas with LSCD (Figure 3A), but goblet cells were not detected.

Histopathological examination

Figure 3B corresponds to the photomicrography of a cornea with LSCD that was stained with TB. The histopathological examination revealed disruptions on the epithelial layer of the cornea and the presence of intensive inflammatory cell infiltration and vessels in the stroma.

Optical anisotropies

The mean OPD was 18.89 ± 3.63 for corneas with LSCD and 14.26 ± 2.41 for controls ($p<0.001$). LSCD was associated with a 24.48% increase in corneal OPD.

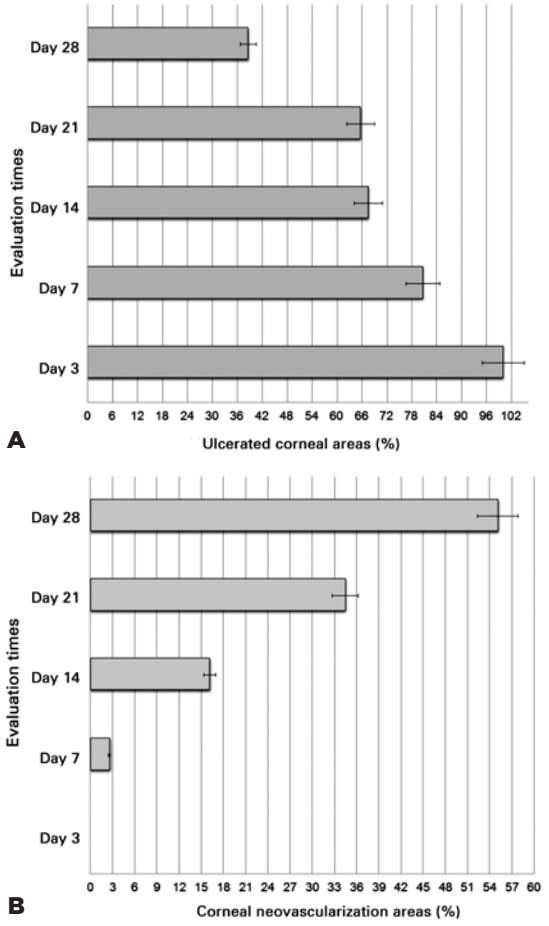

Figure 2. A) Measurements of ulcerated corneal areas (positive fluorescein) performed using ImageJ software. Note that the mean percentage of the ulcerated corneal area decreased over time. B) Measurements of corneal neovascularization areas performed using ImageJ software. Note that the mean percentage of the corneal area covered by vessels increased over time.

Figure 4 demonstrates the absorption curves constructed for corneas with LSCD and controls. $A^{\perp}$ values were higher than $A\parallel$ values for all samples and at all photon wavelengths ($p<0.05$). The stroma of corneas with LSCD showed two polarized light absorption peaks (first at 480 nm and second at 520-560 nm), which coincided with $A^{\perp}$ and $A\parallel$. For controls, a single absorbance peak was observed (520-560 nm). Absorbance values for corneas with LSCD ($A^{\perp}$ range, 0.63-0.93 AU; $A\parallel$ range, 0.45-0.82 AU) were always higher than those for controls ($A^{\perp}$ range, 0.50-0.91 AU; $A\parallel$ range, 0.20-0.61 AU).

LD values calculated for the maximum absorbance peaks of the spectral curves are presented in table 3. LD was negative for all samples. Corneas with LSCD were less dichroic (i.e., they presented a smaller difference between $A\parallel$ and $A^{\perp}$) than controls ($p<0.05$).

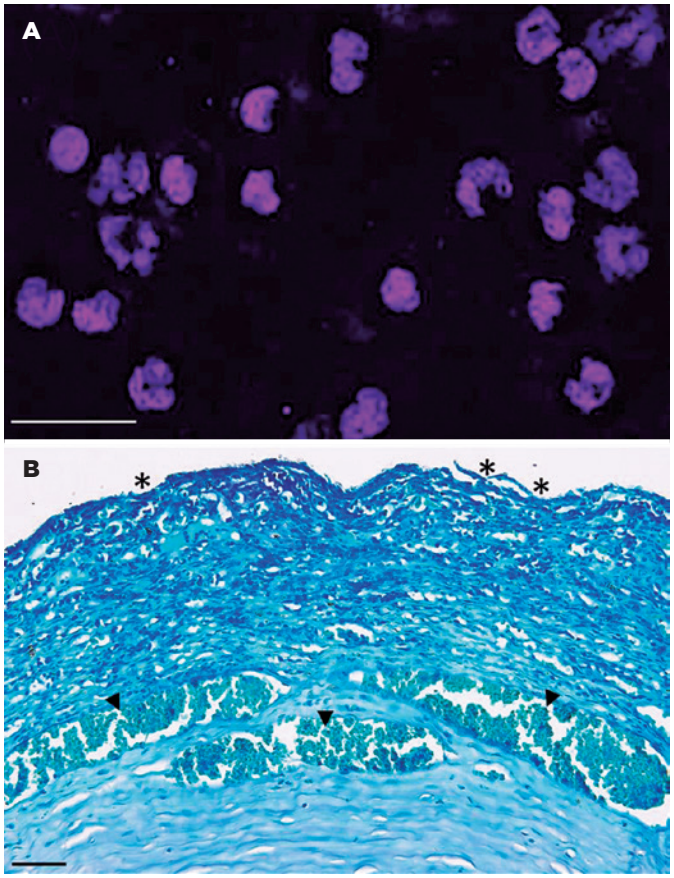

Figure 3. A) Photomicrography of corneal impression cytology collected 28 days after the induction of limbal stem cell deficiency (LSCD). The examination revealed inflammatory cells; however, goblet cells were not detected. The image was processed using ImageJ to eliminate the background and enhance the contour contrast of inflammatory cells. Bar = 20 μm. B) Photomicrography of one section (7 μm) of the cornea that was collected 28 days after the induction of LSCD and evaluated using a light microscope. Note the presence of vessels (arrowheads) and inflammatory cell infiltration in the anterior and middle stroma. The corneal epithelium was disrupted or absent (asterisks). Bar = 50 μm.

DISCUSSION

Ocular injuries characterized by inflammation of the anterior segment can be followed by delayed LSCD[18], which arises from the destruction of limbal stem/progenitor cells or alterations in the corneal/limbal stromal microenvironment. In this investigation, a rabbit model of LSCD was created using a protocol intended to destroy the corneal/limbal epithelium and to disorganize the corneal stroma. All surgical procedures employed for the removal of the corneal/limbal epithelium were done in

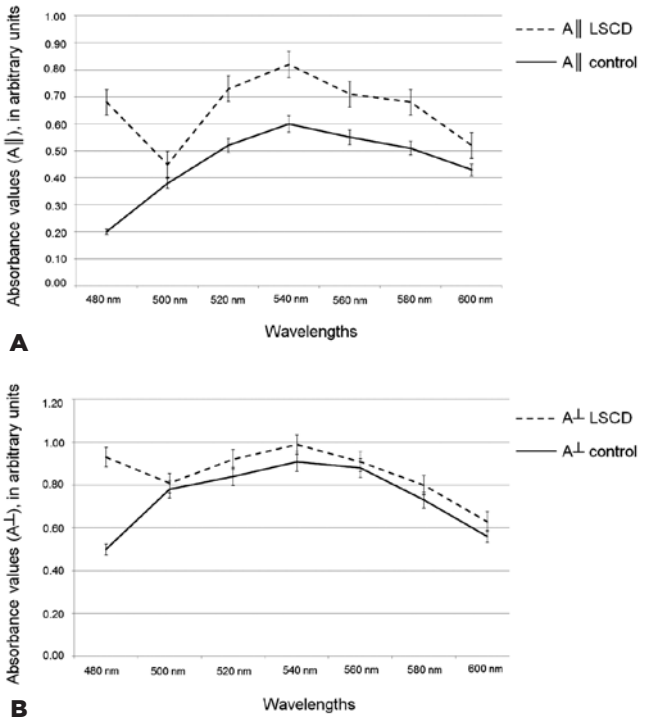

Figure 4. Spectral absorption curves constructed to corneas with limbal stem cell deficiency (LSCD) and to healthy corneas stained with toluidine blue. The parallel absorbance ($A\parallel$) values (A) and the mean perpendicular absorbance ($A^{\perp}$) values (B) were plotted against the different photon wavelengths. Note that absorbance values of corneas with LSCD were always higher than those of controls. $A^{\perp}$ values were higher than $A\parallel$ values for all samples.

Table 3. Linear dichroism for corneas with LSCD and control corneas

Wavelength	Corneas with LSCD	Control corneas
	LD	LD
480 nm	-0.25	---
520 nm	-0.19*	-0.32
540 nm	-0.17*	-0.31
560 nm	-0.03*	-0.33

LSCD= limbal stem cell deficiency; *= $p<0.05$ vs. controls; ---= absent.

consonance with previous studies performed by other groups. The significant difference between our protocol and those from other studies is the agent chosen for corneal chemical burn. While many authors use *n*-heptanol to burn the cornea[16], we used NaOH because it promotes a tissue saponification reaction, causing more severe stromal lesions. We also used NaOH because Andrade et al.[13] demonstrated that *n*-heptanol is associated with a high rate of corneal re-epithelization, which is corroborated by studies conducted by other authors[22].

The clinical features presented by the injured eyes were evaluated for 28 days (4 weeks), which is the usual time interval between the creation of the LSCD model and its use in preclinical studies[19]. All eyes exhibited signs of mild-to-severe inflammation, which is intimately involved in the development of LSCD[18,20]. If inflammatory responses following corneal exposure to alkaline agents are inhibited, it causes a reduction in the appearance of delayed ocular injuries[20].

For many decades, the presence of goblet cells on the corneal surface has been considered the gold standard for diagnosing LSCD[11]. In this work, however, corneal IC did not detect the presence of goblet cells. One possible explanation for this is that corneal IC did not remove all layers of epithelial cells. Furthermore, the accuracy of corneal IC in diagnosing conditions of the corneal surface in animal and humans with LSCD is always complicated, particularly in those who suffer from severe ocular inflammation, in which the proliferation and differentiation of goblet cells are overwhelmingly interrupted[11]. Therefore, the rabbit model utilized herein likely reflects the LSCD phenotype based on four lines of evidence widely used by other authors: diffuse epithelial defects, opacification of the corneal surface, presence of infiltration of inflammatory cells in the cornea, and neovascularization[5,21,22].

Here 10 eyes did not develop a clinical outcome set of LSCD. This is in accordance with other investigations,[22] which have observed that protocols aimed at inducing LSCD may not be 100% effective. However, it is not possible to say if the effectiveness of our protocol was higher or lower than that obtained by authors who used other protocols as the vast majority of studies do not provide quantitative information on the intra-laboratory reproducibility of clinical features. When studying eyes that were injured using the protocol followed in the present study, Andrade et al.[13] observed that all corneas developed epithelial defects and vessels, but severity scores were not attributed to ocular manifestations found. Thus, it remains unclear if the findings from these authors reflect the clinical features of LSCD.

To avoid bias, our rabbits were screened, and only corneas with an outcome set of LSCD were evaluated for optical anisotropies and compared to corneas harvested from eyes free of disorders. Since the discovery of corneal optical anisotropies, many authors have used these phenomena as tools to investigate corneal tissue during various reparative or pathological conditions[6,7]. Optical anisotropy can be accessed in vivo using custom equipment. However, in vivo analyses have disadvantages in relation to analyses made from tissue sections as they provide qualitative data on optical anisotropies, which often require mathematical treatments by matrices or complex vector functions that report on the arrangement space[23,24]. Unfortunately, these matrices do not report on the ordered aggregational state of CFs.

The first type of optical anisotropy (i.e., birefringence) arises from collagen molecular supraorganization within the corneal stroma[6-8,17]. The cornea simultaneously displays intrinsic and form birefringence. Intrinsic birefringence is caused by the orientations and oscillator strengths of all electronic transitions of collagen molecules within corneal tissue[6]. Form birefringence depends on the sub-wave dimension and geometry of the collagen molecule, compatibility of the photon wavelength with the collagen molecule, and packing state of CFs[6]. The technique to evaluate birefringence from water-soaked corneal sections utilized herein provides data on total birefringence, which is the sum of intrinsic and form birefringence[6,17].

Changes in total birefringence brightness intensity established regarding OPD are indicative of alterations in collagen supraorganization[6,7]. In contrast to a previous study[16], which detected loss of stromal lamellar orientation in corneas with LSCD induced by the mechanical debridement of epithelial cells and application of 1-*n*-heptanol, our findings are not suggestive of changes in the spatial orientation of CFs. The results of the present study revealed that LSCD increased the OPD values of rabbit cornea, suggesting that due to the disease, stromal CFs become more crystalline and densely packed than what is observed in control animals. Under pathological conditions, increased packing of corneal stromal CFs has been associated with the development of epithelial defects and loss of corneal transparency[25,26]. Furthermore, as collagen packing and crystallinity are related to the transmission of forces that facilitate cell junction repositioning, diseases that alter the supraorganization

of CFs could compromise mechanotransductive processes, by which mechanical stimuli are translated into intracellular biochemical signs that lead to changes in gene expression[3].

Spectral absorption and LD from sections stained with TB are related to the bioavailability and spatial orientation of glycosaminoglycan (GAG) chains from stromal PGs[6,7,17]. Maximum $A^{\perp}$ and $A^{\parallel}$ values at 520-560 nm photon wavelengths, as presented by corneas with LSCD and controls, have been previously observed in mouse and porcine corneas[6,17]. However, the absorbance peak at 480 nm, as detected only in corneas with LSCD, is a new finding and suggests that GAGs/PGs with differentiated levels of aggregation are available to bind with TB. As a limitation of the present study, we were unable to characterize these GAGs/PGs because comprehensive biochemical analyses were not performed. Despite this, our results corroborate those of other studies that demonstrate alterations in the qualitative expression of GAGs[27] and PGs[28] in debrided corneas.

The negative LD value observed in rabbit corneas stained with TB is similar to that previously reported in mouse and porcine corneas[6,17] and the rabbit limbus[7]. Under conditions that reveal negative LD in the corneal stroma, GAG chains are parallel to the long axis of CFs[6,7,17]. This molecular arrangement model optimizes the ionic interaction between the negative charges of GAG chains and the positive charges of collagen molecules[6]. However, the GAG-collagen interaction is a statistical consideration[17], which can vary due to the highly flexible adaptation of GAG chains to stromal metabolism and the morphofunctional state of the cornea. It is likely that corneas with LSCD were less dichroic (values closer to zero) than controls due to changes in the arrangement of GAG chains.

In conclusion, it was observed that all injured eyes manifested clinical features of inflammation. However, not all injured eyes developed clinical signs consistent with LSCD. Thus, preclinical rabbit models of LSCD must be rigorously screened to ensure experimental homogeneity. LSCD, as induced herein, altered the optical anisotropic properties of rabbit cornea. Knowledge of these changes is important to potentiate strategies aimed at restoring the morphofunctional integrity of the corneal stroma affected by limbal stem cell deficiency.

REFERENCES

1. Cotsarelis G, Cheng SZ, Dong G, Sun TT, Lavker RM. Existence of slow-cycling limbal epithelial basal cells that can be preferentially stimulated to proliferate: implications on the epithelial stem cells. Cell. 1989;57(2):201-9.
2. Dua HS, Saini JS, Azuara-Blanco A, Gupta P. Limbal stem cell deficiency: concept, aetiology, clinical presentation, diagnosis and management. Indian J Ophthalmol. 2000;48(2):83-92. Comment in: Indian J Ophthalmol. 2000;48(2):79-81.
3. Aldrovani M, Filezio MR, Laus JL. A supramolecular look at microenvironmental regulation of limbal epithelial stem cells and the differentiation of their progeny. Arq Bras Oftalmol. 2017;80(4): 268-72.
4. Hayashida Y, Nishida K, Yamato M, Watanabe K, Maeda N, Watanabe H, et al. Ocular surface reconstruction using autologous rabbit oral mucosal epithelial sheets fabricated ex vivo on a temperature-responsive culture surface. Invest Ophthalmol Vis Sci. 2005;46(5):1632-9.
5. Xu B, Fan T, Zhao J, Sun A, Wang RX, Hu XZ, et al. Transplantation of tissue-engineered human corneal epithelium in limbal stem cell deficiency in rabbit models. Int J Ophthalmol. 2012;5(4):424-9.
6. Aldrovani M, Guaraldo AM, Vidal, BC. Optical anisotropies in corneal stroma collagen fibers from diabetic spontaneous mice. Vision Res. 2007;47(26):3229-37.
7. Valdetaro GP, Aldrovani M, Padua IR, Cristovam PC, Gomes JA, et al. Supra-organization and optical anisotropies of the extracellular matrix in the amniotic membrane and limbal stroma before and after explant culture. Biomed Opt Express. 2016;7(12):4982-94.
8. Naylor EJ. Polarized light studies of corneal structure. Br J Ophthalmol. 1953;37(2):77-84.
9. Jan NJ, Grimm JL, Tran H, Lathrop JL, Wollstein G, Bilonick RA, et al. Polarization microscopy for characterizing fiber orientation of ocular tissues. Biomed Opt Express. 2015;6(12):4705-18.
10. Götzinger E, Pircher M, Dejaco-Ruhswurm I, Kaminski S, Skorpik C, Hitzenbrger CK. Imaging of birefringent properties of keratoconus corneas by polarization-sensitive optical coherence. Invest Ophthalmol Vis Sci. 2007;48(8):3551-8.
11. Lim Y, Yamanari M, Fukuda S, Kaji Y, Kiuchi T, Miura M, et al. Birefringence measurement of cornea and anterior segment by office-based polarization-sensitive optical coherence tomography. Biomed Opt Express. 2011;2(8):2392-402.
12. Roth S, Freund I. Second harmonic-generation and orientational order in connective tissue: a mosaic model for fibril orientational ordering in rat tail tendon. J Appl Cryst. 1982;15(1):72-8.
13. Andrade AL, Gomes JA, Luvizotto MC, Perri SH, Campos M. Aspectos clínicos e morfológicos do transplante da membrana amniótica sobre a córnea de coelhos com deficiência induzida de células germinativas do limbo. Vet Zootec. 2009;16(1):127-42.
14. Silva ML, Trujillo DY, Ribeiro AP, Laus JL. Topical 1% nalbuphine on corneal sensivity and epitheilization after experimental lamellar keratectomy in rabbits. Ciênc Rural. 2012;42(4):679-84.
15. Goktas S, Erdogan E, Sakarya R, Sakarya Y, Yilmaz M, Ozcimen M, et al. Inhibition of corneal neovascularization by topical and subconjunctival tigecycline. J Ophthalmol. 2014;2014(2014):452685.
16. Kameishi S, Sugiyama H, Yamato M, Sado M, Namiki H, Kato T, et al. Remodeling of epithelial cells and basement membranes in a corneal deficiency model with long-term follow-up. Lab Invest. 2015;95(2):168-79.
17. Aldrovani M, Vidal BC. Application of principles of optical anisotropies and image analysis to the investigation of molecular packing, crystallinity, spatial organization and three-dimensional topography in collagen fibers from porcine cornea. In: Sanchez PC, editor. Progress in Biopolymer Research. New York: Nova Science; 2007. p. 225-42.

18. Kadar T, Horwitz V, Sahar R, Cohen M, Cohen L, Gez R, et al. Delayed loss of corneal epithelial stem cells in a chemical injury model associated with limbal stem cell deficiency in rabbits. Curr Eye Res. 2011;36(12):1098-107.
19. Selver OB, Durak I, Gürdal M, Baysal K, Ates H, Ozbek Z, et al. Corneal recovery in a rabbit limbal stem cell deficiency model by autologous grafts of tertiary outgrowths from cultivated limbal biopsy explants. Mol Vis. 2016;22:138-49.
20. Amir A, Turetz J, Chapman S, Fishbeine E, Meshulam J, Sahar R, et al. Beneficial effects of topical anti-inflammatory drugs against sulfur mustard-induced ocular lesions in rabbits. J Appl Toxicol. 2000;20 Suppl 1:S109-14.
21. Afsharkhamseh N, Ghahari E, Eslani M, Djalilian AR. A simple mechanical procedure to create limbal stem cell deficiency in mouse. J Vis Exp. 2016;(117) doi:10.3791/54658.
22. Parente DR, Silva MR, Silva Junior RG, Marques MA. Experimental models of limbal stem cell deficiency in rabbits - clinical study. Arq Bras Oftalmol. 2002;65(2):153-60.
23. Jaronski JW, Kasprzak HT. New polarimetric method for in-vivo measurement of corneal birefringence. In: Proceedings of SPIE - the International Society for Optics and Photonics Engineering. 1998. p.187-90.
24. Hitzenberger CK, Götzinger E, Pircher M. Birefringence properties of the human cornea measured with polarization sensitive optical coherence tomography. Bull Soc Belge Ophtalmol. 2006;(302):153-68.
25. Höllhumer R, Watson S, Beckingsale P. Persistent epithelial defects and corneal opacity after collagen cross-linking with substitution of dextran (T-500) with dextran sulfate in compounded topical riboflavin. Cornea. 2017;36(3):382-5.
26. Chakravarti S, Petroll WM, Hassell JR, Jester JV, Lass JH, Paul J, et al. Corneal opacity in lumican-null mice: defects in collagen fibril structure and packing in the posterior stroma. Invest Ophthalmol Vis Sci. 2000;41(11):3365-73.
27. Soriano ES, Campos MS, Michelacci YM. Effect of epithelial debridement on glycosaminoglycan synthesis by human corneal explants. Clin Chim Acta. 2000;295(1-2):41-62.
28. Soriano ES, Campos MS, Aguiar JA, Michelacci YM. Effect of epithelial debridment on human cornea proteoglycans. Braz J Med Biol Res. 2001;34(3):325-31.